

Electrosynthesis of symmetrical aramid oligomers

C. Chevrot*

Laboratoire de Recherches sur les Polymères et les Matériaux Electroactifs, Université Paris Nord, ESCOM, 13 bd de L'Hautil, 95092 Cergy Pontoise, France

and T. Benazzi

Laboratoire de Recherches sur les Macromolécules (UA 502 CNRS), Université Paris Nord, 93430 Villetaneuse, France

and M. Barj

Laboratoire de Spectrochimie Infra-rouge et Raman (UPR 2631), Université de Lille 1, 59655 Villeneuve d'Ascq Cedex, France

(Received 21 June 1993; revised 14 July 1994)

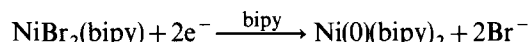
Symmetrical aramid oligomers have been synthesized by dehalogenative polycondensation of two aryl dibromides containing primary amide structural units as monomers in the presence of electrogenerated zerovalent nickel acting as a catalyst. As the oligomers obtained were insoluble in organic solvents, they were characterized by solid-state n.m.r. spectroscopy, infra-red spectroscopy and elemental analysis. Analysis of the monomer and oligomer samples by X-ray diffraction shows that these symmetrical materials possess a better crystallinity than the related unsymmetrical compounds.

(Keywords: aramid oligomer; electrosynthesis; crystallinity)

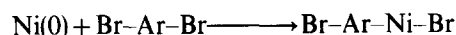
INTRODUCTION

Owing to the high strength and high thermal resistance of aromatic polyamide fibres such as poly(*p*-phenylene terephthalamide) and poly(*m*-phenylene isophthalamide), numerous studies of the synthesis and properties of these materials have been described^{1–4}. The reaction between a dicarboxylic aromatic acid dichloride and an aromatic diamine constitutes the main synthetic method that has been used^{1–4}. Furthermore, some aromatic polyamides can lead to liquid crystalline solutions in certain solvent systems². Various other methods of synthesis of aromatic polyamides with high molecular weights have been recently used^{5–7}, and a particular mention should be made of the synthesis of aromatic oligo-(or poly)amides from monomers containing amide structural units^{8,9}. In these latter cases, the synthesis is based on the activation of a carbon halide bond by zerovalent nickel acting as a catalyst, and leads to a coupling polymerization of the aromatic-dihalide-containing amide group. We have shown previously⁸ that dehalogenative polycondensation of 4,4'-dibromo-[(*p*-biphenylene)amide] (DPBA), in the presence of electrogenerated zerovalent nickel (in catalytic amounts), leads to the corresponding polymer, but with a low molecular weight. The main advantage of this method is to give a regular polymer containing *p-p* linkages. First, the NiBr₂(bipy) complex (where bipy is 2,2'-bipyridine) is electrochemically reduced to give

zerovalent nickel, Ni(0), as follows:



Then, this Ni(0) species is inserted into the C–Br bond of the monomer, thus leading to the formation of an oxidative addition complex, as follows:



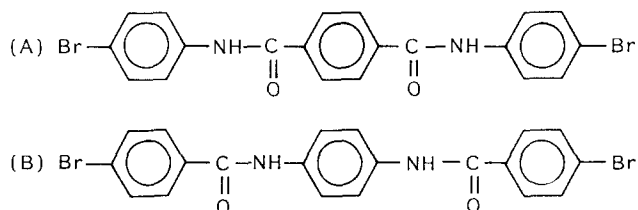
Finally, coupling between this complex and a further Br–Ar–Br species gives the required polymer^{8,10–14}. We have already used NiBr₂(bipy) as a catalytic precursor in order to synthesize various polyconjugated compounds^{10–16}. These materials can be obtained in powder form^{10–15}, as well as in thin layers deposited onto conducting substrates^{13,16}. The use of this precursor does not imply any cathodic reduction of the oxidative addition complex as similar behaviour is observed for other organometallic Ni(II) complexes^{17–20}.

Ueda *et al.*⁹ have synthesized four semiaromatic polyamides from aryl dichlorides containing secondary amide structural units as monomers by using powdered zinc as a reducing agent for the nickel(II) salt catalytic precursor.

We report in this paper the synthesis of aramid oligomers from symmetrical aryl dibromides containing amide groups by using the dehalogenative polycondensation process mentioned above. It was found that use of an unsymmetrical monomer such as DPBA has two drawbacks. First, the reactivities towards zerovalent

* To whom correspondence should be addressed

nickel of the two carbon–bromine bonds in the monomer are quite different, thus inducing a chemical coupling with an irregular structure. Secondly, both the asymmetry of the monomer molecule and the irregular chain structure that is obtained are disadvantages when trying to obtain crystalline material. Therefore, we have synthesized the two symmetrical monomers, A and B, (see below) in order to examine if the corresponding polymers show better crystallinities than poly[4,4'(*p*-biphenylene)amide].



The crystallinities of the polymers that were obtained were examined by using X-ray diffraction.

EXPERIMENTAL

Reagents

The $\text{NiBr}_2/2,2'$ -bipyridine complex ($\text{NiBr}_2(\text{bipy})$) was prepared as previously described^{10–14}. *N,N*-dimethylacetamide (DMA), which was used as the solvent for electrosynthesis, was distilled under reduced pressure over calcium dihydride. The supporting salts (LiBF_4 , LiClO_4) were dried under vacuum at 120°C for 24 h. Toluene was distilled over calcium dihydride, while the others reagents and solvents were purchased commercially and were used as received.

4-Bromoaniline was purified by sublimation under vacuum to give a white product (m.p. = 66–67°C; literature²¹ gives 66.4°C). Terephthaloyl dichloride was recrystallized from hexane to produce white needles (m.p. = 83°C; literature²² gives 83–84°C). 1,4-Diaminobenzene was recrystallized from water, and then dried under vacuum at 50°C, while protecting from light, to give white crystals (m.p. = 144°C; literature²¹ gives 140°C). 4-Bromobenzoyl chloride (Aldrich) was used without purification (m.p. = 42°C; literature²¹ gives 42°C). The last four compounds were characterized by using ^1H n.m.r. spectroscopy.

Synthesis of monomer A

To a solution of 4-bromoaniline (0.12 mol) in toluene (25 ml) was added dropwise a solution of terephthaloyl dichloride (0.05 mol) in toluene (50 ml). A white solid was formed immediately. The mixture was stirred for 1 h at 30°C, after which the product was filtered, washed with acid water, water and diethyl ether, and dried. Recrystallization from ethanol gave white needles (yield = 90%). The purified product was characterized by ^1H n.m.r. and i.r. spectroscopy (see below). Elemental analysis: calculated C 50.63, H 2.95, N 5.91, Br 33.75%; found C 50.57, H 3.05, N 5.93, Br 33.87%.

Synthesis of monomer B

To a solution of 4-bromobenzoyl chloride (0.045 mol) in dry ether (25 ml) was added dropwise a solution of

1,4-diaminobenzene (0.02 mol) in dry ether (20 ml). A white product precipitated at once. After stirring the mixture for 1 h at room temperature, the product was filtered, washed with an alkaline solution and acetone and then dried. Recrystallization from ethanol gave a white product (yield = 89%). The purified product was characterized by ^1H n.m.r. and i.r. spectroscopy (see below). Elemental analysis: calculated C 50.63, H 2.95, N 5.91, Br 33.75%; found C 50.54, H 3.09, N 5.68, Br 32.87%.

Electrochemical processes

The electropolymerization of monomers A and B was carried out in DMA under an argon atmosphere by using either LiBF_4 or LiClO_4 as supporting electrolytes. The electrolyses were performed with a Tacussel Radiometer apparatus (PJT 35-2 potentiostat, GSTP4 generator, IG5-N coulometer) connected to a Sefram (TGM 101) X Y recorder. A jacketed cell with two compartments separated by a glass-sintered disc was utilized. A continuous stirred mercury pool was used as the working electrode (cathode), polarized against a saturated calomel electrode (SCE) as reference, with a magnesium cylinder being the counter-electrode. In a typical experiment, 1 mmol of catalyst (either without, or with an excess of 2 bipy/ $\text{NiBr}_2(\text{bipy})$) and 2 mmol of monomer were added to a mixture of 30 mmol of electrolyte in 100 ml of DMA. Electrosyntheses were carried out in the potentiostatic mode, with the applied potential being determined from the cyclic voltammogram plotted on glassy carbon as the working microelectrode (see ref. 8). The resulting solution, containing a light brown precipitate, was then poured into an aqueous sulfuric acid solution (5 wt%). The solid was separated by filtration, washed with water and diethyl ether and then dried in vacuum at 80°C. Argentimetric titration of the aqueous phase with silver nitrate yielded the amount of bromide released during the electrolysis process.

I.r. and n.m.r. spectroscopy

I.r. spectra were obtained by using a Perkin–Elmer 580 spectrometer, while n.m.r. spectra were recorded on a Bruker AC 200 spectrometer (200 MHz).

Melting point measurements

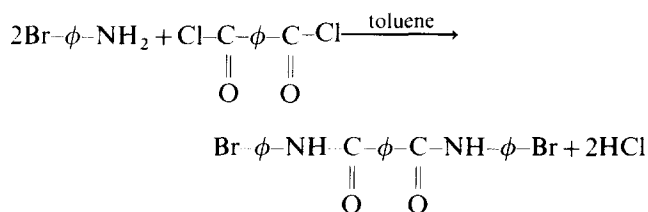
Melting points were measured by using a Buchi 510 apparatus.

RESULTS AND DISCUSSION

Synthesis and characterization of monomers

The two monomers, A and B, were easily synthesized in good yield according to the following reactions:

monomer A



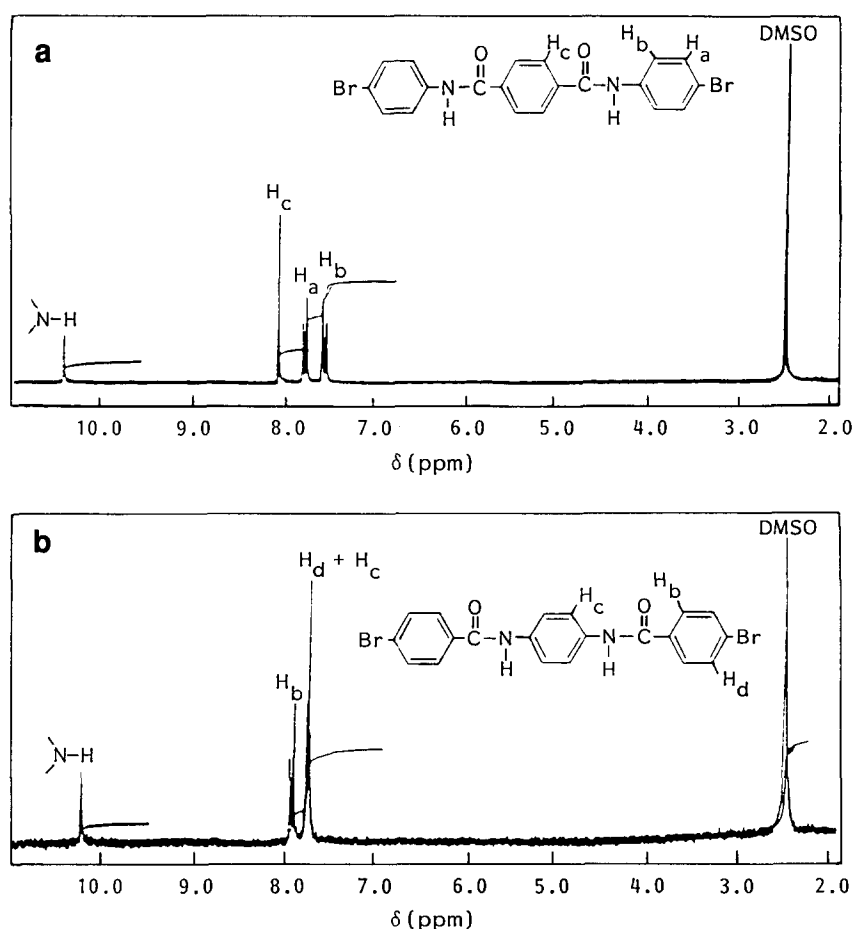
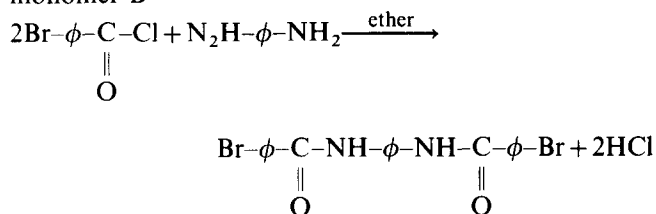


Figure 1 ^1H n.m.r. spectra of monomer A (a) and monomer B (b) in deuterated DMSO

monomer B



Characterization of these two monomers has been carried out by using ^1H n.m.r. and i.r. spectroscopy and the spectra obtained are shown in Figures 1 and 2.

In the ^1H n.m.r. spectra of each monomer, all of the protons have been identified (see Figure 1). We can see that the spectra of the two monomers are quite different, as a result of the inverse linkage of the amide group.

The i.r. spectra of each monomer reveal the presence of the main absorption bands, with the N-H stretching vibrations occurring at 3325 cm^{-1} for monomer A and at 3310 cm^{-1} for monomer B. In both cases, the strong absorption band near 1640 cm^{-1} is related to the amide I band (the carbonyl absorption). The positions of these two bands are characteristic of strong hydrogen bonding interactions between the carbonyl and N-H groups. Finally, the strong amide II band occurs at 1525 cm^{-1} for monomer A, and as a broad band near 1530 cm^{-1} for monomer B. Furthermore, we also obtained a sharp absorption peak near 820 cm^{-1} . This latter signal is characteristic of C-H out-of-plane vibrations of the 1,4-disubstituted phenyl ring.

Electrosynthesis and characterization of polymers

As previously described^{8,10-14}, the electrosynthesis reactions were carried out on a mercury pool in the potentiostatic mode, at the reduction potential of the catalytic precursor, $\text{NiBr}_2(\text{bipy})$. At the beginning of the electrolysis, the solution turns deep green, the characteristic colour of zerovalent nickel in the presence of bipy. At the same time the current intensity quickly decreases. After a few minutes, the solution becomes red and then gradually begins to darken, while the current intensity becomes stable until the end of the reaction, at which point the intensity again quickly decreases. The faradic yield reaches 95%, with this figure being based on the theoretical charge calculated in order to carry out the reaction. During the electrolysis a precipitate is formed; after separation and further treatment, this solid was characterized by ^{13}C solid-state n.m.r. and i.r. spectroscopy. However, due to the insolubility of the polymers in all of the solvents used, high resolution ^1H n.m.r. could not be used to characterize the samples.

Details of the electrosynthesis process are presented in Table 1: as monomer B is of a lower purity than monomer A, we have only carried out one electrosynthesis experiment in this case. This did, however, give similar results to that obtained for monomer A.

The amount of Br^- released is increased when no excess of bipy is used in the electrosynthesis; as a consequence, the *DP* value of the isolated product increases. Simultaneously, we can notice a reduction in the yield of the oligomer that is obtained.

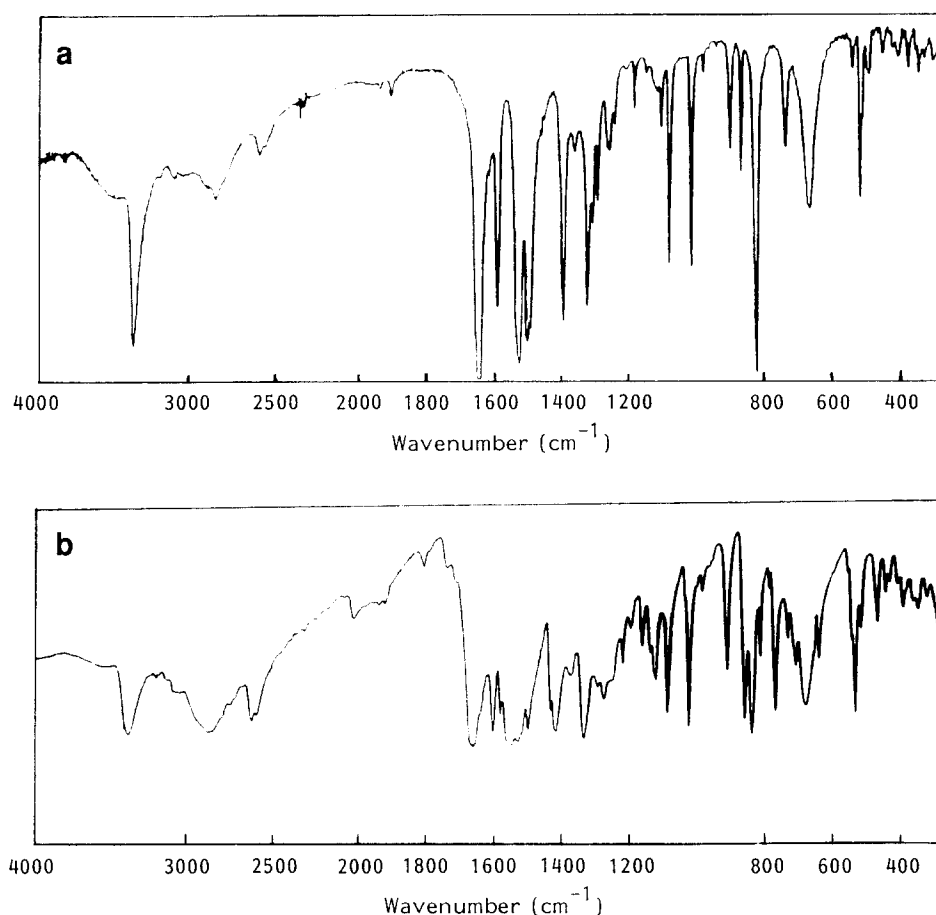


Figure 2 I.r. spectra of monomer A (a) and monomer B (b) (KBr pellets)

Table 1 Details of the electrosynthesis processes used in this study; 2 mmol of monomer used in each case

Monomer	A	A	B	A	A
Electrolyte	LiBF ₄	LiBF ₄	LiBF ₄	LiClO ₄	LiClO ₄
Catalyst ^a	1	2	1	1	2
Br ⁻ released ($\times 10^{-3}$ mol) ^b	4.2	5.2	4.9	3.7	5.6
Weight of isolated product (g)	0.68	0.52	0.63	0.72	0.54
Yield (%)	71	55	66	75	57
Analysis ^c					
C	67.6	69.34	66.5	66.82	70.02
N	7.8	8.13	7.94	7.68	8.28
H	4.88	4.97	5.27	5.13	4.92
Br	12.39	6.97	8.8	11.21	6.32
DP ^d	~4	6-7	4-5	4	7

^a Catalyst systems used: (1) NiBr₂(bipy)/bipy = 10^{-3} mol/ 2×10^{-3} mol; (2) NiBr₂(bipy) = 10^{-3} mol (no excess bipy used)

^b Theoretical amount of Br⁻ is 6×10^{-3} mol

^c Calculated values; C 76.43, N 8.92%

^d Estimated value, based on the presence of one bromine atom at each chain end

¹³C solid-state n.m.r. did not allow us to differentiate structurally between the two polymers (see *Figure 3*). Indeed, both polymers show the same five peaks in the aromatic carbon range; in addition, the chemical shift range examined (124.3 to 136.8 ppm) is narrower than the values predicted from calculations using data obtained from solution studies²³.

Moreover, we observe that the carbon of the amide

group is characterized by a signal occurring near 165 ppm, for both polymers. Such results were not unexpected as the linkage between the two aromatic rings on the polymer backbone strengthens the structural similarity of the two products.

The solid-state n.m.r. spectra of the corresponding monomers are also shown in *Figure 3*, where it can be seen that the spectra are quite different. Thus, although

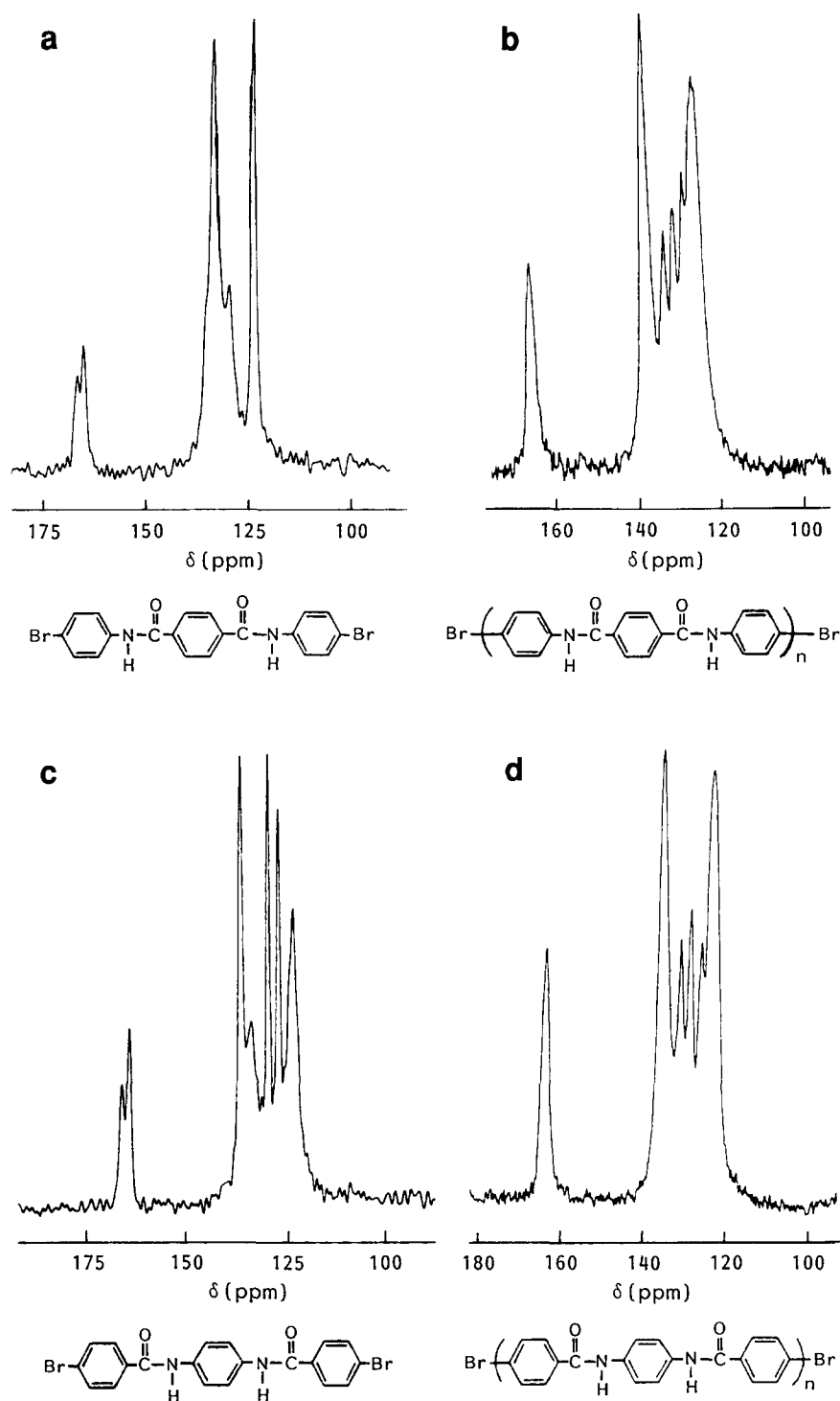


Figure 3 ^{13}C solid-state n.m.r. spectra (200 MHz) of both sets of monomers and polymers: (a) monomer A; (b) polymer A; (c) monomer B; (d) polymer B

the carbon of the amide group gives the same doublet for the two monomers A and B (near 164 and 166 ppm, respectively), the number and position of the peaks are different in the aromatic range. From calculations of the chemical shifts using data obtained from solution studies²³, it appears to be very difficult to assign each peak to a specific carbon. Table 2 summarizes the theoretical chemical shifts of the six different aromatic carbons.

More signals can be detected for monomer B than for monomer A. Furthermore, as in the case of the polymers,

the aromatic carbon range (124.4–137.3 ppm for monomer A and 123.7–133.2 ppm for monomer B) is narrower than the predicted range. Therefore, we observe a significant downfield shift for carbons 1 and 3 (monomer A) and for carbon 6 (monomer B) compared to the calculated values. This means that the hydrogen bonding interactions detected in the i.r. spectra of the monomers produce a clear deshielding of the above carbons. This shift is induced by an increase in the positive charge of the carbon of the amide group, thus leading to an increase in the withdrawing effect.

Characterization by i.r. spectroscopy (Figure 4) indicates that the absorption bands already described for the two monomers are also observed for the corresponding polymers. However, at least two typical differences should be noted. First, there is a strong decrease in the strength of the band near 1075 cm^{-1} in the polymer spectrum when compared with that of the corresponding monomer. The decrease in this band, generally attributed to the

Table 2 Calculated chemical shifts of the aromatic carbons in monomers A and B, with data taken from solution studies²³

<div style="display: flex; justify-content: space-around; align-items: center;"> <div style="text-align: center;"> <p>Monomer A</p> </div> <div style="text-align: center;"> <p>Monomer B</p> </div> </div>			
	δ (ppm)		
Carbon	Monomer A	Monomer B	
1	117.0	125.3	
2	131.7	131.2	
3	120.1	128.9	
4	138.1	132.8	
5	137.0	134.0	
6	127.1	118.8	

C-Br vibration mode in the phenyl ring at a chain end²⁴, could explain both the reduction in the Br content and the increase in the degree of polymerization. The second difference concerns the absorption band for the C-H in-plane deformation. For the monomer, we observe a characteristic peak near 1012 cm^{-1} , while in the polymer three weak peaks appear at 1018, 1010 and 1003 cm^{-1} . As previously described⁸, the peak at 1010 cm^{-1} can be assigned to the C-H in-plane deformation of *p*-disubstituted phenyl groups at the chain ends. The presence of this peak requires the existence of a C-Br bond at the chain end. In addition, in the low frequency regime, the intensity of the observed mode at $\sim 510\text{ cm}^{-1}$ seems to decrease significantly for both oligomers A and B. This confirms the presence of C-Br bonds at the chain ends. The two other weak peaks could be attributed to the C-H in-plane deformation of the two other 1,4-disubstituted phenyl rings in the polymer (oligomer) backbone.

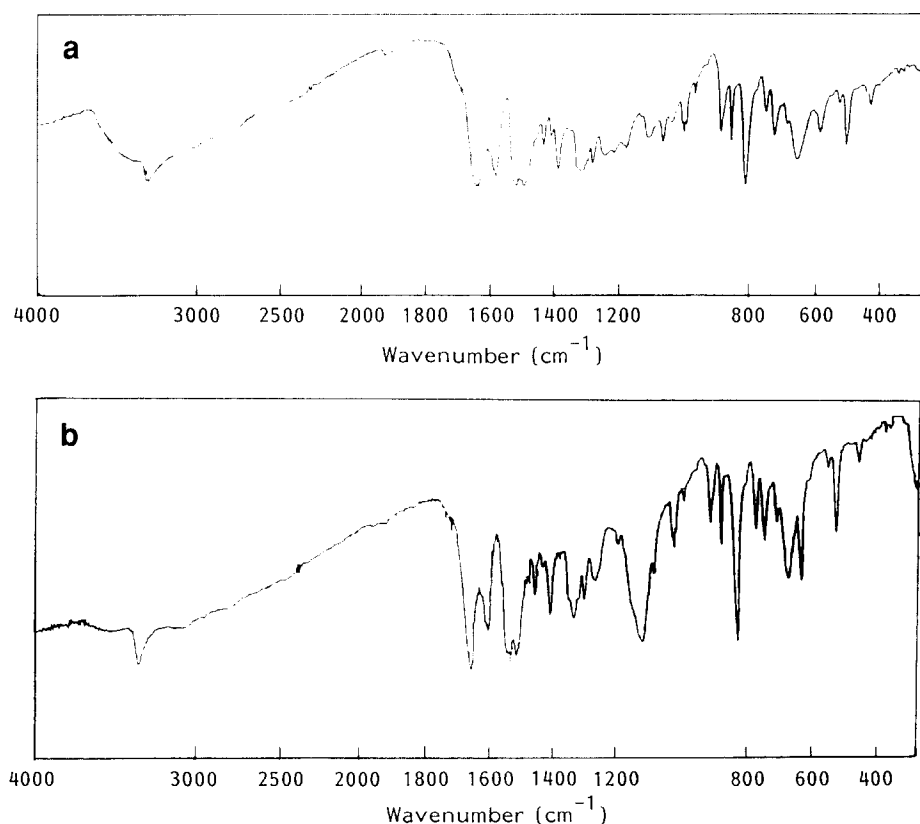
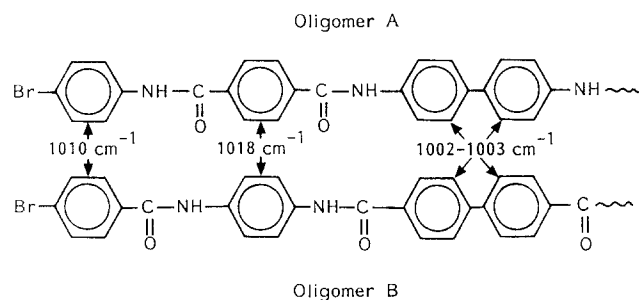


Figure 4 I.r. spectra of polymer A (a) and polymer B (b) (KBr pellets)

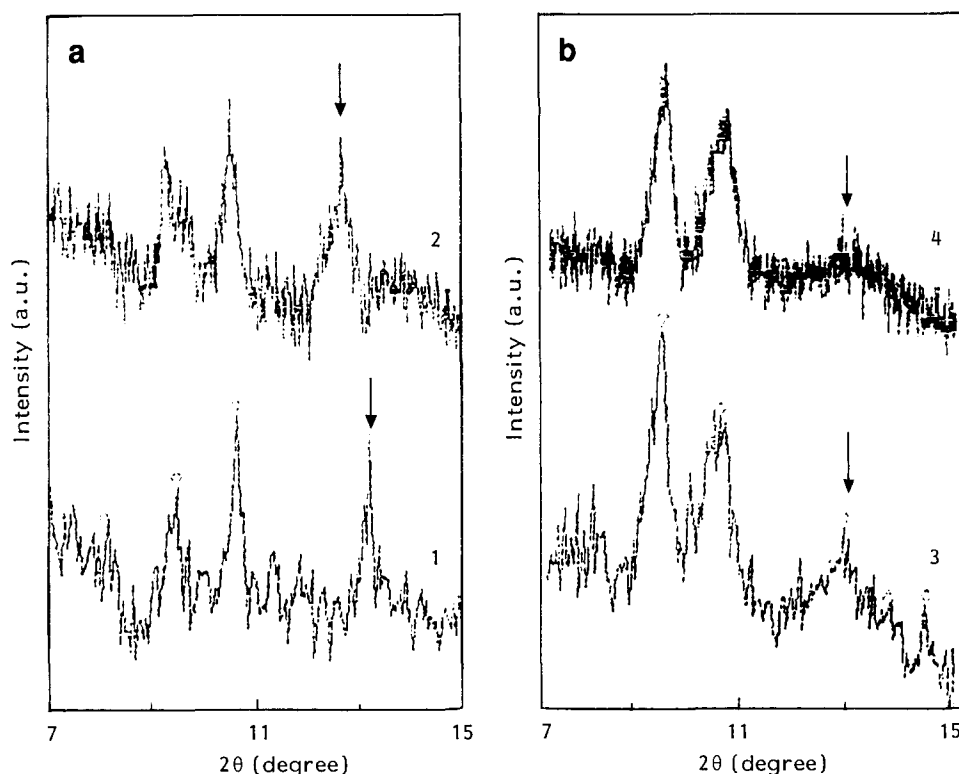


Figure 5 X-ray diffraction patterns of: (1) monomer A; (2) oligomer A; (3) monomer B; (4) oligomer B

According to the i.r. spectrum of poly(1,4-phenylene terephthalamide)²⁵, the C–H in-plane deformation of the 1,4-disubstituted phenyl ring occurs at 1019 cm^{-1} , while the C–H in-plane deformation of the other 1,4-disubstituted phenyl ring at $1002\text{--}1003\text{ cm}^{-1}$ is close to that observed for poly[4,4'-(*p*-biphenylene)amide]²⁶, occurring at 1005 cm^{-1} for the latter. These assignments have been made in the light of a normal mode analysis which was carried out on a number of benzanilide compounds²⁷.

X-ray diffraction of monomers and polymers

The X-ray diffraction diagrams of monomer and oligomer powders were obtained using a Siemens diffractometer connected to an AT computer, with Zr filtered $\text{MoK}\alpha$ radiation ($\lambda = 0.7093\text{ \AA}$) being used in the 2θ goniometer configuration.

Figure 5 shows the X-ray diffraction diagrams obtained for the monomers and the corresponding oligomers. As observed for similar compounds^{28,29}, these only exhibit a few Bragg reflections between $2\theta = 9\text{--}13^\circ$, corresponding to reticular distances close to 4.3, 3.8 and 3.2 \AA . The intensity of the diffraction peak corresponding to the shortest distance decreases significantly in the case of oligomer B. This could be associated with a structural change, probably involving chain orientation and/or symmetry effects.

The crystallinity of these materials is assumed to be high. The degree of crystallinity is usually estimated from the ratio of the integrated intensities of the amorphous and Bragg diffraction parts of the experimental X-ray pattern. In our case, no significant diffusion background (associated with an amorphous halo) is observed. The crystallinity is thus assumed to be high for both types of materials.

However, a qualitative comparison of the diffraction diagrams suggests that both the B monomer and oligomer could have higher crystallinities than the corresponding A compounds. This is confirmed by the observation of better resolved i.r. spectra for the B compounds, when compared to the corresponding A materials.

The profiles of the diffraction peaks for both the B monomer and oligomer seem to be wider ($2\theta = 0.5^\circ$) than those of the A compounds, which probably indicates that their crystallite sizes are much smaller than those of the latter compounds. It is usually possible to estimate the crystallite size from that part of the peak broadening which is due to the size effect by using the so-called Sherrer formula. Using silicon powder as a standard, the instrumental broadening, measured from the 111 diffraction peak ($2\theta = 12.98^\circ$), is found to be $\sim 0.2^\circ$. For our monomers and oligomers, the 'true' broadening due to the size effect is ~ 0.1 and 0.3° for A and B, respectively. The corresponding crystallite sizes are, respectively, ~ 520 and 170 \AA .

ACKNOWLEDGEMENTS

The authors are greatly indebted to J. P. Lere-Porte (University of Montpellier II) for obtaining the solid-state n.m.r. spectra and to F. Drisch (ESCOM, Cergy Pontoise) for very helpful discussions and suggestions.

REFERENCES

- 1 Morgan, P. W. *Macromolecules* 1977, **10**, 1388
- 2 Morgan, P. W. *J. Polym. Sci. Polym. Symp.* 1985, **72**, 27
- 3 Preston, J. and Hofferberg, W. L. *J. Polym. Sci. Polym. Symp.* 1978, **65**, 13
- 4 Vollbracht, L. in 'Comprehensive Polymer Science' (Eds G. Allen

- and J. C. Bevington). Vol. 5, Pergamon, Oxford, 1989, p. 375
- 5 Yoneyama, M., Kakimoto, M. and Imai, M. *Macromolecules* 1988, **81**, 1908
- 6 Otuki, T., Kakimoto, M. and Imai, M. *J. Polym. Sci. Polym. Chem. Edn* 1989, **27**, 1775
- 7 Turner, S. R., Perry, R. J. and Blevins, R. W. *Macromolecules* 1992, **25**, 4819
- 8 Chevrot, C. *Eur. Polym. J.* 1990, **26**, 127
- 9 Ueda, M., Ito, T. and Seino, Y. *J. Polym. Sci. Polym. Chem. Edn* 1992, **30**, 1567
- 10 Siove, A., Ades, D., Chevrot, C. and Froyer, G. *Makromol. Chem.* 1989, **190**, 1361
- 11 Ngbilo, E., Ades, D., Siove, A. and Chevrot, C. *Polym. Bull.* 1990, **24**, 17
- 12 Siove, A., Ades, A., Ngbilo, E. and Chevrot, C. *Synth. Met.* 1990, **38**, 331
- 13 Faid, K., Ades, D., Chevrot, C. and Siove, A. *Makromol. Chem. Macromol. Symp.* 1991, **47**, 377
- 14 Chevrot, C., Riou, M. T. and Froyer, G. *Synth. Met.* 1993, **55**, 4783
- 15 Aboukassim, A., Siove, A., Ades, A. and Chevrot, C. *Synth. Met.* 1989, **33**, 57
- 16 Aboukassim, A., Faid, K. and Chevrot, C. *J. Appl. Polym. Sci.* 1994, **52**, 1569
- 17 Schiavon, G., Bontempelli, G., Magno, F. and Daniele, S. *J. Electroanal. Chem.* 1982, **140**, 91
- 18 Fauvarque, J. F., Petit, M., Pfluger, F., Jutand, A., Chevrot, C. and Troupel, M. *Makromol. Chem. Rapid Commun.* 1983, **4**, 455
- 19 Aboukassim, A., Pelous, Y., Chevrot, C. and Froyer, G. *Polym. Bull.* 1988, **19**, 595
- 20 Froyer, G., Pelous, Y. and Chevrot, C. *J. Electroanal. Chem.* 1992, **37**, 159
- 21 'CRC Handbook of Chemistry and Physics' (Ed. R. C. Weast), 71st Edn, CRC Press, Boca Raton, FL, 1990-1991
- 22 Greenwood, T. D., Kahley, R. A. and Wolfe, J. F. *J. Polym. Sci., Polym. Chem. Edn* 1980, **18**, 1047
- 23 Breit-Maier, E. and Voelter, W. '¹³C NMR Spectroscopy', VCH, Weinheim, 1978, pp. 213-214
- 24 Yamamoto, T., Yamamoto, A. and Hayashi, Y. *Bull. Chem. Soc. Jpn* 1978, **51**, 2091
- 25 The infra-red spectrum of an authentic sample of poly(1,4-phenylene terephthalamide) was kindly provided by E. I. du Pont de Nemours
- 26 Zappia, E., Tosi, G., Cardellini, L. and Sandrolini, F. *Mater. Chem.* 1981, **6**, 73
- 27 Kim, P. K., Hsu, S. L. and Ishida, H. *Macromolecules* 1985, **18**, 1905
- 28 Xu, D., Okuyama, K., Kumamaru, F. and Takayanagi, M. *Polym. J.* 1984, **16**, 31
- 29 Koga, K., Ueta, S. and Takayanagi, M. *Polym. J.* 1988, **20**, 639